SEARCHING FOR STRUCTURE IN THE RINGS OF SATURN K.-M. Aye, L. W. Esposito, LASP, University of Colorado, 3665 Discovery Drive, Boulder, CO, USA (michael.aye@lasp.colorado.edu)

Introduction Data from the Cassini mission have shown that the rings of Saturn are much more dynamic in their behavior than it was known after the Voyager observations. While Saturn's tidal force and collisions limit accretion [1], occultation profiles of the edges of the rings from Cassini's UVIS instrument show wide variability, indicating perturbations by local mass aggregations. The timescales for aggregation and disaggregation inferred by observations range from hours to months and this collective behavior of the ring particles can be described by a mass-based predator-prey system as described in [2]. We present a study testing out several signal processing methods for identifying oscillations near the strongest spiral density waves that fit either the description of straw-like features as identified in [3] or that of Lindblad resonances as investigated by our group in [4].

Data In the current work, image data from the Saturn orbit injection (SOI) phase of Cassini's Imaging Science Subsystem (ISS) are being analyzed. These data have some of the highest resolution for Saturn rings of the Cassini mission. A calibration and filtering pipeline based on the Integrated Software for Imagers and Spectrometers (ISIS) software toolkit of the United States Geological Survey (USGS) has been set up and published as an open source Python-based library called "pyciss" [5].

Part of this pipeline is projecting the ring data into a Saturn-centered cylindrical coordinate system (see Fig. 2) based on the navigation data of the Cassini spacecraft as recorded by SPICE kernels of NASA's NAIF group. The advantage of projecting the images into a cylindrical coordinate system is that the azimuthally symmetric structure of the rings are stored as parallel features that can easily be integrated for better signal to noise ratios of any feature being studied.

Method 1: Measure of azimuthal dispersion along radius With this method we want to test the hypothesis that clumping in the rings can be identified by changes in the statistical dispersion of the photo-metric signal in ISS images along the azimuth when compared at different radii of the rings. Because some of the pixels of the ISS CCD are prone to be outliers even after applying the calibration routine of ISIS ("CISSCAL 3.6"), a simple standard deviation per radius row of the CCD array could be heavily biased by these outliers.

We therefore apply a more robust median-based variance measure of dispersion called "*median absolute deviation*" (MAD), which is defined as the median of the absolute deviations from the data's median, i.e.

$$MAD = median_i \left(|X_i - median_j \left(X_j \right) | \right) \qquad (1)$$

with $X_1, X_2, \ldots, X_n$ a uni-variate data set. The MAD value has therefore a similar relationship to the *median* value as the *standard deviation* has to the *mean*; it also has previously been applied to gray-scale and color image analysis before, e.g. in [6]. Figure 2 shows the result of applying the MAD estimator to an SOI image with a strong spiral density wave signature. In general, the row-based dispersion increases at the location of the most intense density waves. A zoomed-in view reveals

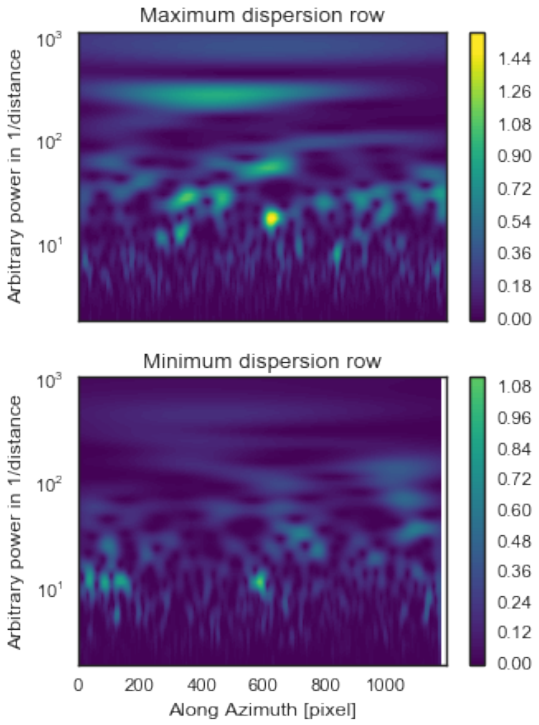

Figure 1: A very preliminary wavelet analysis on the 2 image rows with minimum and maximum statistical dispersion along the ring azimuth, as identified per the right-hand side of Figure 2. The powers and x-axis values are arbitrary in value at this point, but the scale at which a power is drawn relates to the x-axis as 1/pixel-size. A potentially significant difference in the power distribution can be noted.

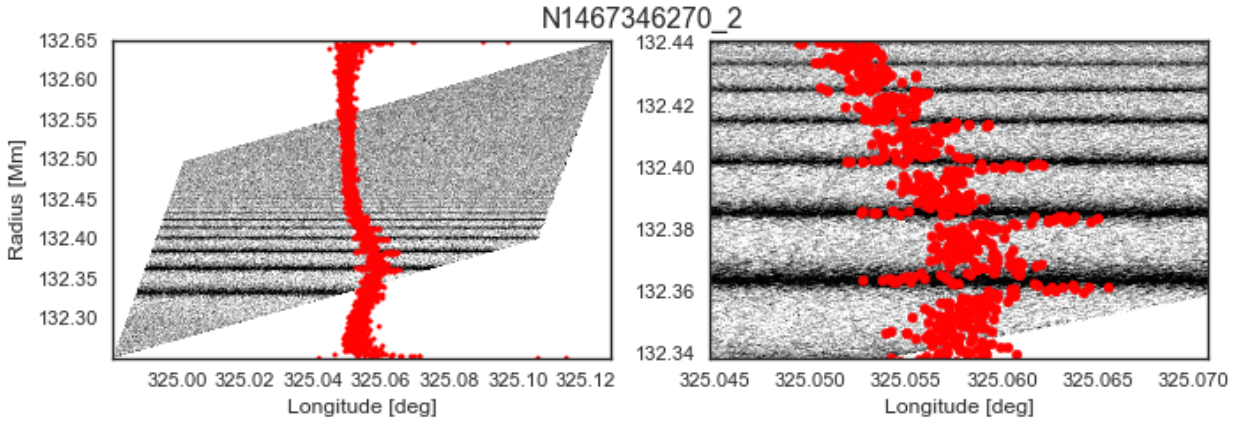

Figure 2: Applying the robust dispersion estimator "median absolute deviation" to each row of the cylindrically projected ring image. The values of the MAD estimator are drawn — arbitrarily shifted above the image for comparison — as red scatter points with lower values towards the left. A general increase of variance at the location of the biggest spiral density waves is visible, centered around radius 132.37 Mm. The right-hand plot shows a zoom-in that reveals that the dispersion is asymmetrically distributed around the crests of the density wave. The data was taken on 2004-07-01T03:46, with an emission angle of approx. 117° (with values larger than 90 indicating an observation of the un–lit side of the rings).

however, that the values of dispersion are asymmetrically distributed around the crests of the density waves (with the crests being the dark parts of the image, due to observed extinction on the un-lit side of the rings in this data). Starting from the inner edge of a density wave, the crest of the density wave (crests are dark on the unlit side of the rings due to the increased extinction) first shows a local minimum of dispersion. Then a local maximum after the crest shows up, followed by average values and finally the largest values of dispersion per density wave appearing right before the next crest. This pattern is visible over several waves.

Status: At this stage we can state that this pattern has been found with several SOI images. Prior to the LPSC conference we will cross-check the locations of these events against the known Lindblad resonance locations. It should be noted that the signature of "straw" like structure shows a collective approximately similar orientation of elongated elements that could not easily be identified using this method. However, currently ongoing studies of very high resolution UVIS occultation data [7] finds oscillatory signatures near spiral density wave crests as well

Method 2: Wavelet analysis As discussed in [8], a classical windowed Fourier transform represents an inaccurate and inefficient method of time-frequency localization, as it imposes a scale or response interval T into the analysis. For analyses where a predetermined scaling may not be appropriate because of a wide range of dominant frequencies, a method of timefrequency localization that is scale independent, such as wavelet analysis, should be employed [8]. Figure 1 shows a very preliminary example of applying a wavelet analysis to the previously identified interesting rows of minimum and maximum statistical dispersion rows in Figure 2.

Status The azimuthal pixel resolutions need to be worked out for the wavelet analysis so that one can make a statement on the power that is existent in what length scale. We will show further progress for this at the conference.

Method 3: Sinusoidal fits We will follow up another hypothesis before the conference: the fitting of sinusoidal functions to each row of the cylindrically projected ring data should have smaller residuals where oscillations caused by moons or clumping appear in the photometric data.

References: [1] Karjalainen, R and Salo, H. *Icarus*, 172:328–348 (2004). [2] Esposito, LW et al. [3] Porco, CC et al. *Science*, 307:1226–1236 (2005).
[4] Rehnberg, M et al. *AAS*, 47:#104.04 (2015).
[5] Aye, KM. *pyciss* (2015).
doi:10.5281/zenodo.34134. [6] Khalil, HH et al.
[7] Brown, Z et al. *AAS/DPS Meeting Abstracts* (2015).
[8] Torrence, C and Compo, GP. *Bulletin of the American Meteorological Society*, 79:61–78 (1998).